PROCEEDINGS, 51st Workshop on Geothermal Reservoir Engineering
Stanford University, Stanford, California, February 9-11, 2026
SGP-TR-230

Development of Integrated Numerical Model with Naturally Fractured Reservoir Principles of Salak Geothermal Field

Iqbal Kurniawan, Peter, Muhamad Ridwan H., Mulyadi, Frederick T. Libert, and Gede K.D.S Giri

Star Energy Geothermal Salak. Wisma Barito Pacific II 17th-21st Floor Jl. Letjen. S. Parman Kav. 60, Jakarta 11410, Indonesia

qliw@starenergy.co.id

Keywords: Numerical model, naturally fractured reservoir, model calibration, initial state, history matching, forecast.

ABSTRACT

The Salak Geothermal Field is currently the largest operating geothermal field in Indonesia and has been continuously operating since 1994, with an installed capacity of 405.4 MWe, comprising of 388.8 MWe flash plant and 16.6 MWe binary plant. As one of the country's most mature geothermal fields, Salak has drilled more than 115 wells and accumulated an extensive dataset through drilling and reservoir monitoring programs. Leveraging this dataset, Salak's Earth Science team has updated the static model by incorporating the latest drilling result, monitoring data, new reservoir studies, including new insights from the Naturally Fractured Reservoir (NFR) study. This updated static model served as the foundation for updating the Salak numerical model, with the objective of making the numerical model to have consistent reservoir property distributions. In addition to updating the static property distributions, the dynamic boundary conditions were also revised to align with the updated conceptual model of the field. These improvements made the NFR-based numerical model more effective during the calibration process and demonstrated high calibration quality during the pre-exploitation condition and reservoir response throughout commercial production, including recent major injection strategy change, namely the Salak Injection Realignment Program (SIRP). The quality result from the calibration process indicates that the model is reliable to predict the evolution of key dynamic reservoir parameters observed from surveillance activities during the first few years of the SIRP. Overall, the model update using the NFR-based data has improved the calibration results and enhanced confidence in the model as a reliable predictive tool for evaluating various long-term exploitation strategies, which ultimately improve decision-making quality for Salak's key strategic projects.

1. INTRODUCTION

The Salak (Awibengkok) Geothermal Field, located about 70 km south of Jakarta in West Java, is the largest operating geothermal field in Indonesia with an installed capacity of 405.4 MW, consisting of 388.8 MWe flash plant and 16.6 MWe binary plant. Commercial production commenced in 1994 when Units 1 and 2 (each 55 MW) were put into service, followed by Units 3/4/5/6 in 1997 (each 55 MW). Units 4/5/6 were uprated to 65.6 MW in 2004, to 67 MW in early 2022, and to 69.6 MW in mid-2025; Units 1/2/3 were uprated to 60 MW in 2005. Furthermore, the binary plant, with an installed capacity of 16.6 MWe, was commissioned in May 2025. Star Energy Geothermal Salak Ltd. (SEGS) supplies steam to Units 1/2/3 (owned by the state utility company PLN and operated by its subsidiary PT Indonesia Power), while Units 4/5/6 and binary plant geothermal energy supply and electricity generation facilities are operated by SEGS. To date, more than 115 wells have been drilled, including producers, brine and condensate injectors, and monitoring wells from early exploration, development, and infill wells drilling campaigns in the following years.

Salak reservoir is a high-temperature, liquid-dominated system with benign chemistry and low-to-moderate non-condensable gas (NCG) content (Acuna et al., 1997). The hottest measured temperature in the reservoir is ~620°F (327°C) identified from a deep well located in the southwestern sector near the major upflow. Several minor upflow "hot spots" are identified in the central, eastern, and southeastern areas. Convective and often nearly isothermal pre-exploitation temperature profiles were found in the main production area (Rohrs et al., 2005) with general temperature trend declines from West to East Salak. Based on the distinction of reservoir temperature, fluid chemistry, tracer response, and pressure trends four production cells are recognized in Salak reservoir—West, Central, East, and Far East—(Rohrs et al, 2005).

The initial state pressure in Salak was defined based on early exploration data from wells drilled in 1982-1986 with the majority of data align on a common pre-exploitation pressure gradient of 0.355 psi/ft (Strobel, 1986). Complemented by the result of pressure interference test, Salak reservoir seems to have pressure communication throughout the field. Prior to exploitation, the reservoir was predominantly occupied by liquid except near the very top of the commercial resource where a low pressure and temperature two-phase region overlie the shallow portion of the reservoir (Rohrs et al., 2005).

The fluid flow preferentially trends north-northeast, outflowing at surface thermal manifestations located at the northern margin, with some fluids moving to the east-southeast exiting at surface thermal manifestations near the eastern margin. The permeable entries are aligned with the northeast-trending maximum horizontal stress (SHmax) which allows the fluid to move preferably and quickly in this direction and are consistent with the northeast-trending fracture system delineated from microearthquake (MEQ) swarms (ES Salak, 2017).

From a stratigraphic perspective, the field has several subsurface rocks comprised of andesitic and basaltic lavas, breccias, tuffs, and lahar consisting of several long-lived volcanic centers along the southwestern margin of Mount Salak (Hulen and Lutz, 1999; Stimac and Sugiaman, 2000; Stimac et al., 2008). Four major formations are recognized, listed from oldest to youngest: (1) the Lower Volcanic Formation, composed of marine sediments and volcaniclastic units (MSV) together with lower andesite; (2) the Rhyodacite Marker (RDM); (3) the Middle Volcanic Formation; and (4) the Upper Volcanic Formation. The Middle and Upper Volcanic Formations consist of stacked dacitic units at their bases, overlain by andesitic rocks (Aprilina et al., 2017). Additionally, numerous intrusions are distributed throughout the Salak/Awibengkok geothermal field. Figure 1 illustrates the general flow of hot fluids including the location of each well pad and four production cells identified in Salak, which provides a general description of the conceptual model elements used in the numerical modeling process.

Intensive reservoir surveillance programs and integration of new data from infill drilling have provided validation and any necessary update of the conceptual model to properly understand the key reservoir parameters contributing to the production performance of Salak reservoir. In 2020-2021, the Earth Science Team developed a new static model incorporating recent data obtained from drilling result, monitoring data, base of reservoir study, and new knowledge from the Naturally Fractured Reservoir (NFR) study. NFR study aimed at analyzing and interpreting available well feedzones that resulted in the distribution/characterization of downhole permeability, direct fracture characterization, structural analysis, and analog study. This study provides the basis for determining fracture permeability, spacing, and anisotropy distribution in Salak reservoir as input for the updated static model.

This new and improved static model is expected to provide a more robust reservoir properties for the new Salak numerical model, critical for making a more accurate forecasts for evaluating SEGS major organic growth opportunities and major reservoir management projects, such as the on-going injection realignment to improve the long-term Salak reservoir performance.

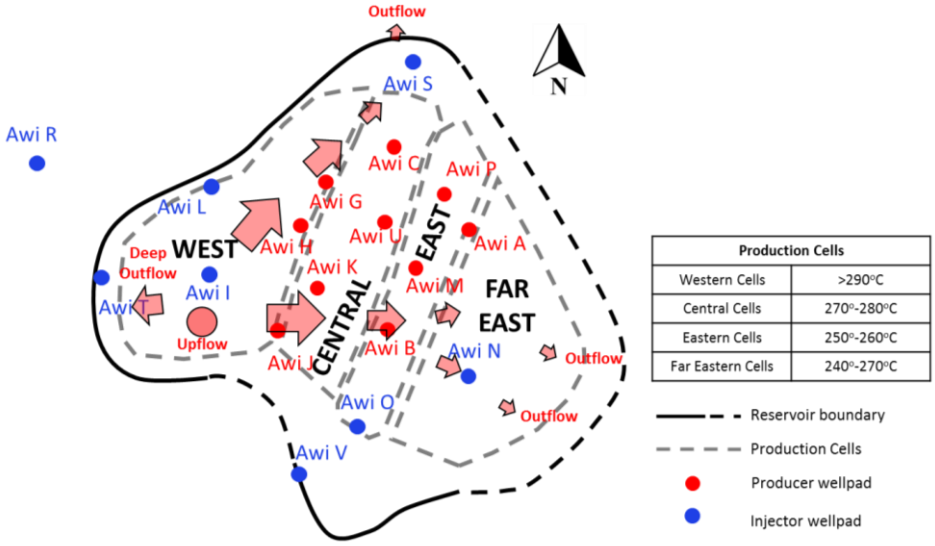

Figure 1: Map showing the general hot fluid flow in Salak, including pad locations and the four production cells, modified after Golla et al. (2020).

2. NUMERICAL MODEL PROPERTIES AND SETUP

2.1 Model Container, Gridding, and Layering

The bulk model volume refers to the new interpretation of the top and base of the connected fracture network, following Aprilina et al. (2021). The connected fracture network corresponds to the transitional conductive-convective temperature regime where permeability is relatively low, while still allowing possible external aquifers connection for fluid inflow and outflow. The top of the connected fracture network, which defines top of model geometry, coincides with the base of conductive temperature and onset of propylitic alteration (first epidote), and the base, which delineates bottom of model geometry, is constrained by injection-induced MEQs and MEQ density. Those together constitute the bulk volume of reservoir used in the numerical model. The reservoir domain is discretized into regular, cubic shaped simulation cells “grid blocks” oriented NE, consistent with the major distribution of dip magnitude of open and effective fracture that is also parallel with the SHmax tectonic stress orientation (Aprilina, 2021 and Salak AMT, 2015). The grid size was homogenously distributed in lateral direction with 200 m x 200 m. According to Pasikki et. al. (2019) this relatively coarse discretization is appropriate because dual porosity formulation generates small fracture elements while geothermal wells typically have high productivity. Completing wells with high flow rates in too small fracture elements can lead to computational inefficiency and numerical instability. The vertical discretization varies from 100-200 m, with finer layering near the Ryodacite Marker (RDM) and Middle Dacite Formations to adequately capture liquid level movement and enthalpy changes at shallow to moderate depth. In total, the model has dimensions of 49 × 47 in X-Y direction with 37 layers, this consists of 31 active layers with approximately 18,000 actives grid blocks that further partitioned into 61,000 blocks using combination of MINC 2 and 4 formulation. The model structure is summarized in and is depicted by figure 2.

Table 1: Summary of Salak new model structure and dimension.

Parameter	Description
Grid Orientation	Oriented to NE
Grid shape and dimension	Regular cubes with 200 m × 200 m
Vertical layering	100 m to 200 m, finer near liquid level
Active grid blocks	~18,000 further partitioned to 61,000 using MINC 2-4

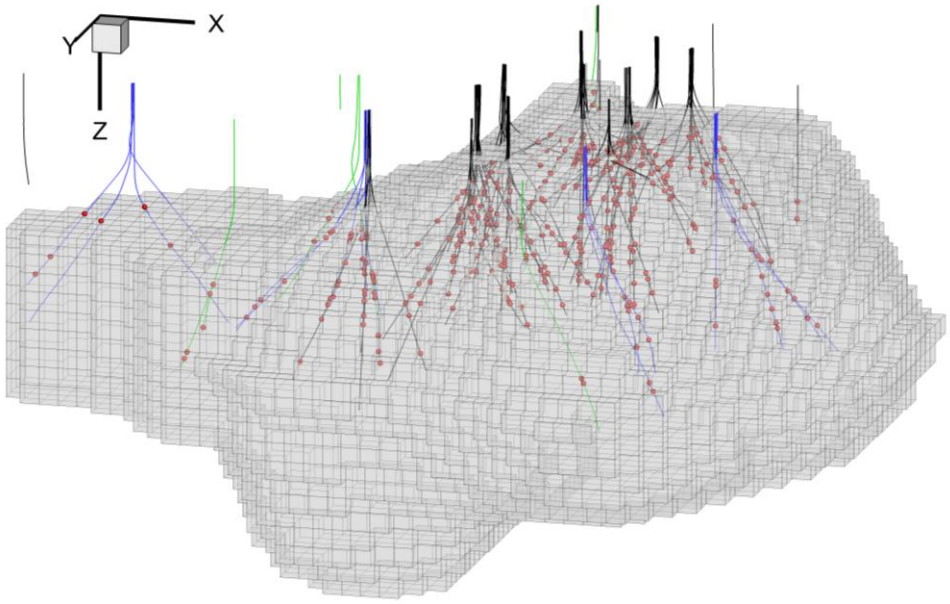

Figure 2: Container structure (bulk volume) of Salak numerical model with regular lateral grid geometry and variable vertical discretization.

2.2 Static Property Distributions

The initial static property distribution refers to the study of Aprilina et al. (2021) discussing about Salak new static model that incorporated recent data and is based on naturally fractured reservoir principles. The static property was then further calibrated during initial state modeling and production history matching to finally match all focused parameters needed during calibration process.

2.2.1 Fracture Porosity, Fracture Permeability and Permeability Barriers

Fracture porosity governs fluid stored in the fracture, although most of the pore volume of the fractured system resides in the matrix. A typical value of 1% fracture volume relative to bulk volume was used in this model. On the other hand, fracture permeability has significant impact on controlling the ability of fractures to transmit fluids and control the major flow in the reservoir. An improved approach called cumulative average and residual PI' modeling, was applied in the updated static model. More than 280 calibrated productivity indices (PI'; PI corrected to eliminate the effects of mobility and reservoir enthalpy) from individual feed zones were used as basic data to derive the value of fracture permeability. The PI' values range from 1.4×10^{-4} to 8×10^{-3} kph.cuft.cp/lb/psi with the majority of feedzones located in middle andesite formation. The analysis of the PI' was started by constructing the background model to capture global vertical and horizontal fracture permeability trend without including details from well data, followed by generating residual models to account for the difference between the background model and well data. Both background and residual models were developed using the kriging method. The combination of background and residual models defines the final fracture permeability distribution for numerical modeling. Vertically, fracture permeability value is decreasing with increasing depth, while horizontally, the distribution was assigned based on directional ratios from the Salak anisotropy study by Nordquist (2017), showing higher permeability in the Y (NE–SW) direction than in the X (NW–SE) direction ($k_y / k_x = 2.5$), consistent with the SHmax orientation of the Salak Field. Figure 3 shows the fracture permeability value at Y (NE-SW) direction versus cumulative frequency of bulk reservoir volume.

In Salak numerical model, vertical permeability barriers were introduced to honor the nature of Salak reservoir where it was divided into 4 production cells i.e. West, Central, East, and Far East. Moreover, a horizontal permeability barrier was also imposed near Ryodacite Marker (RDM) zone to reduce the mass transfer and heat transported by mass in vertical directions.

2.2.2 Fracture Spacing

Fracture spacing governs the size of matrix-fracture interfacial area that will provide control on the ability of mass and heat exchange between the matrix and fractures. It is a key parameter in determining the capacity of the rock mass to reheat the injectate and play an important role in the long-term performance of wells in water dominated reservoir like Salak. Together with matrix permeability and external recharge, the fracture spacing is adjusted to match observed pressure drop and microgravity. Fracture spacing distribution was based on borehole image logs and fracture frequency or spacing of effective fractures from the PTS logs. In general, the fracture spacing trend shows increasing with depth and decreasing from south to north with p10 to p90 value ranges from 360 to 900 ft. Higher value of fracture spacing is required in area where thermal breakthrough has occurred, this will limit the ability of the injectate fluid to be conductively heated by the rock matrix. Figure 3 indicates the calibrated fracture spacing value against the cumulative frequency of bulk reservoir volume.

2.2.3 Matrix Porosity and Permeability

Matrix porosity is a parameter affecting the amount of fluid stored in the pore volume of the reservoir while matrix permeability affects the matrix-fracture connectivity and exchange of fluids-heat between them. Approximately more than 200 core samples data were used in constructing the matrix property model. Lithologic units were grouped into 5 petrophysical groups (PGs) based on petrophysical properties, depositional styles, and hydrothermal alteration. This includes fine pyroclastic, coarse pyroclastic, lava, intrusion and marine sediments. Their proportion in each formation was utilized to estimate the weighted average matrix property value for each identified formation, namely, upper dacite, upper andesite, middle dacite, middle andesite, RDM, lower andesite, MSV, and intrusion. Figure 3 depicts the populated data representing the calibrated range value of weighted matrix porosity and permeability against cumulative frequency of bulk reservoir volume.

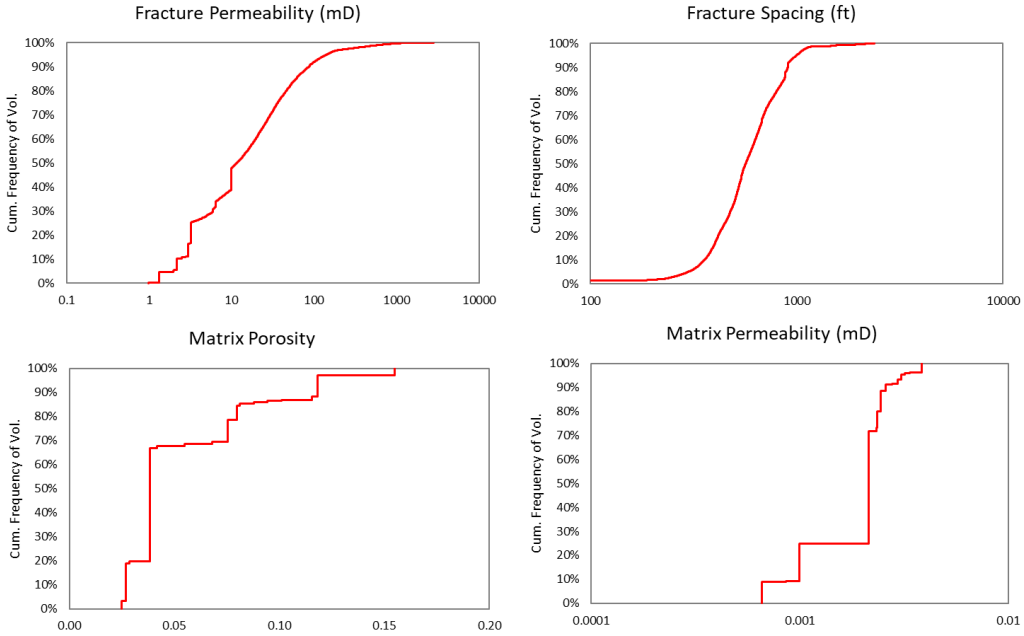

Figure 3: Calibrated static property values from the new Salak model, based on naturally fractured reservoir principles, plotted against the cumulative frequency of bulk reservoir volume.

2.2.4 Other Parameters

To properly capture the behavior of fractured reservoir, the numerical model employs two permeable media i.e. matrix and fractures. The matrix acts as fluid storage that contains most of pore space but has low permeability, while fractures provide high permeability for major fluid flow at low pore volume. Those two elements are connected through matrix-fracture connection parameters.

Based on the lesson learned from process-modeling of thermal recovery near injection well in Salak, Multiple Interacting Continua (MINC) formulation was implemented to capture cooling effects near and far away from the injection wells. This approach is used to avoid the overestimation of reservoir capacity to heat up injected fluid, thus, the model could capture the slow thermal recovery near the injection wells and thermal breakthrough impact near the production wells. The process modeling indicated that MINC 4 should be assigned to properly capture the thermal recovery effect in the main area of interest, while MINC 2 was applied elsewhere to optimize computational efficiency. Another parameter set was the fluid-rock interaction represented by Grant's Curve with residual liquid and steam saturation of 30% and 5% respectively.

2.3 Boundary Condition

2.3.1 Top and Bottom Boundary

The uppermost and lowermost model cells are connected to the large, impermeable boundary grid blocks held at constant temperature, atmospheric at the top and 350ºC at the bottom boundary. These blocks serve as conductive heat sink and source in the model. Distances to these boundaries vary with local top of reservoir elevation and the interpreted base of the reservoir.

2.3.2 Upflow, Outflow, and Aquifers

Natural convective recharges are situated in several locations referring to conceptual model of Salak. It is represented by major upflow in the southwest (highest measured temperature at Salak ~620°F / 327°C) and several minor upflows "hot spots" in the east, southeast, and north, consistent with measured well data and initial geochemical model interpretations. The upflow is implemented as high-enthalpy hot liquid injection totaling approximately 492 kph (62 kg/s), with enthalpy ranging from 640 – 740 BTU/lb (1,500–1,700 kJ/kg).

The major upflow in the southwest has preferentially moved north-northeast and outflowed at K. Parabakti and Sarimaya located in the north of Salak. Some fluid outflow occurs east-southeast toward surface thermal manifestations complex at Cibeureum and K. Cipamatutan. These outflows are represented by mass discharging out of the reservoir from the uppermost blocks at the respective locations with total mass of approximately ~11 kg/s.

Three hot, constant-pressure aquifers located to the north, south, and westernmost Salak at elevation -2,000 ftasl (pressure ranges from 1,500 to 2,000 psi) serve as outfield injection location and, as pressure declines, could act as mass sources during history matching. Two cold, constant-pressure aquifers in the east and central areas at elevations of 1,500 to 1,700 ftasl (pressure ranges from 450 to 950 psi) represent cold fluid influx to model the marginal recharge identified near the area. Figure 4 indicates the location of boundary conditions in Salak model.

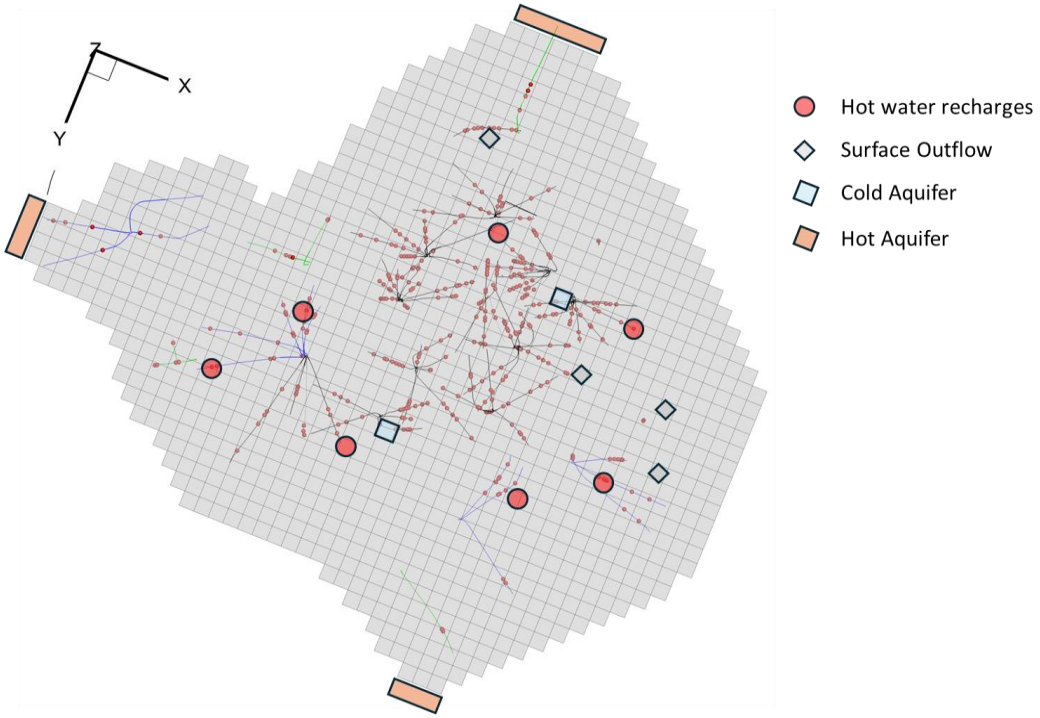

Figure 4: Illustration showing the Spatial distribution of hot waters recharges, surface outflow, cold aquifer, and hot aquifers in Salak numerical model.

3. NUMERICAL MODEL CALIBRATION

3.1 Initial State Modeling

After setting up the model and boundary condition, the initial state runs were performed for ~150,000 years, this timescale was considered as appropriate for this model to reach steady state condition as marked by the stable pressure and temperature profile over time as well as balanced net mass and energy changes in the system. This timescale for each model varies and is influenced by reservoir size, permeability structure, and magnitude of boundary conditions specified in the model. The initial state modeling provides the general depiction of initial pressure, temperature, and fluid saturation distribution in the reservoir with satisfactory fit between the model and measured data as implied by 5-10% Normalized Root Mean Square (NRMSE).

Calibration focused on several parameters including upflow location and strength, fracture permeability distribution, and other boundary conditions. Measured initial pressure derived from early exploration wells drilled in 1982-1986 are well matched by the model as indicated in figure 5. Furthermore, pre-exploitation temperature interpreted primarily from stable measured temperature surveys before 1998. The model was calibrated using 52 initial temperature datasets with good agreement across all production cells, the typical temperature match is shown in figure 6-7. Figure 8 illustrates the initial state temperature distribution showing the hot fluid upflowing in the southwestern area with preferential northeastward flow consistent with the conceptual model. In the pre-exploitation state, the reservoir was largely filled with liquid except possibly near the very top of the commercial resource in the eastern area, a low temperature and low-pressure two-phase region overlie the shallowest portion of reservoir. This is consistent with steam and gas kicks during drilling of some wells in AWI A-1, E-3, F-1, and M-5 and by the presence of Cibeureum fumarole in southeast of Salak (Rohrs et al., 2005). The modeling result as portrayed in figure 9 reproduces a small two-phase region in east or southeast area, consistent with this observation.

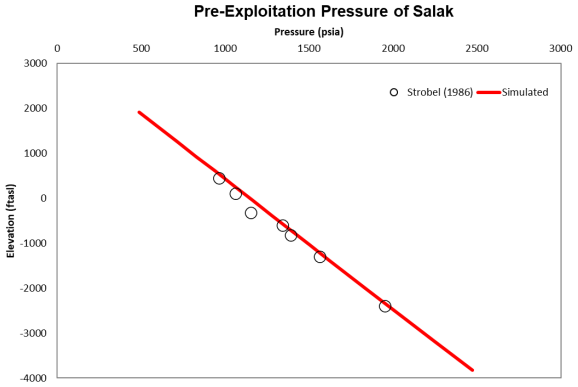

Figure 5: The model reproduces the observed pre-exploitation pressure distribution with good agreement.

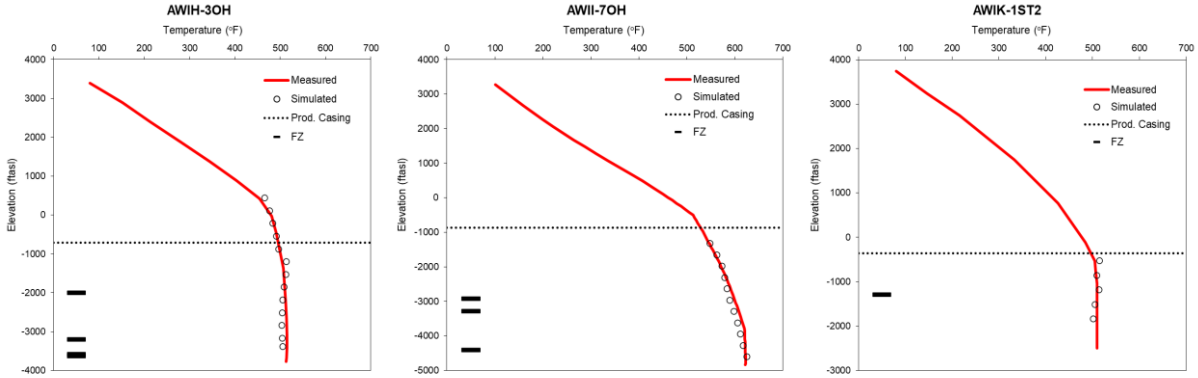

Figure 6: Initial temperature match in West and Central Production Cells, indicating good agreement with actual data.

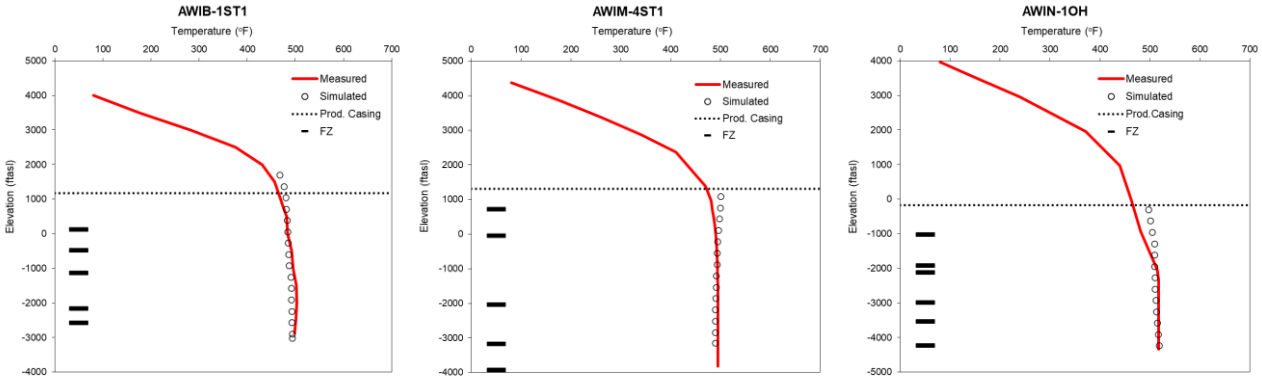

Figure 7: Initial temperature match in East and Far East Production Cells, indicating good agreement with actual data.

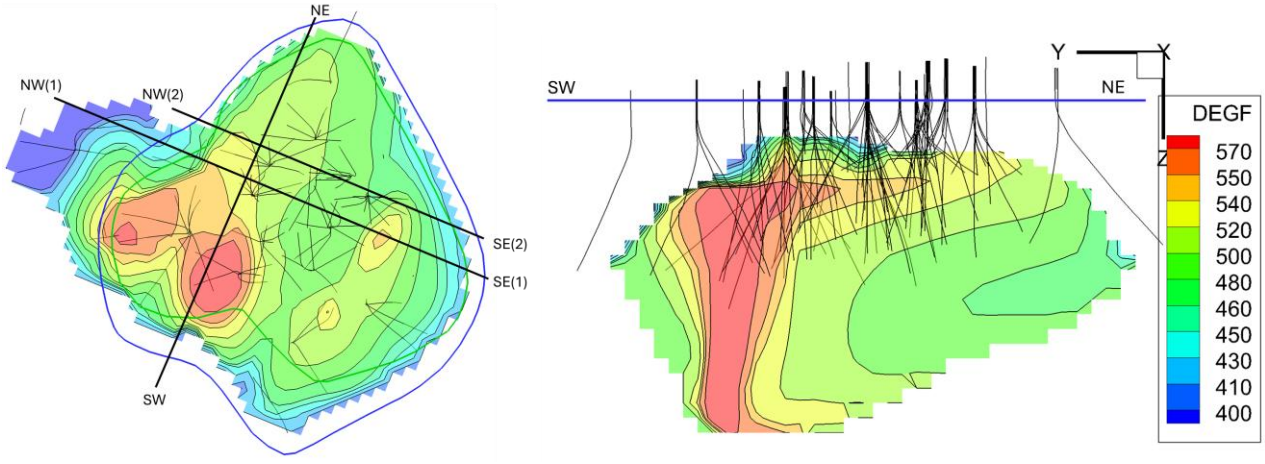

Figure 8: Initial temperature distribution in the Salak reservoir model, showing a major hot fluid upflow in southwest Salak and northeastward flow consistent with the conceptual model.

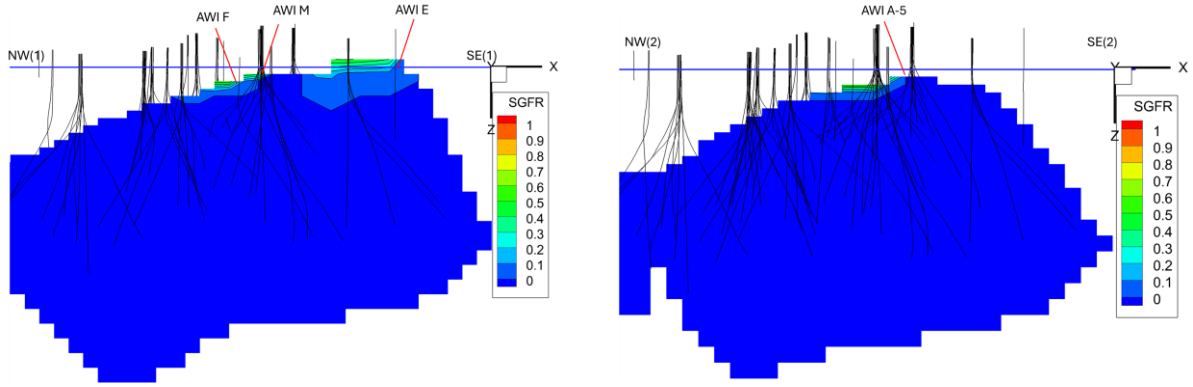

Figure 9: Initial fluid saturation distribution in the Salak reservoir model. The low-pressure, low-temperature two-phase zone in the uppermost Eastern area is accurately captured by the model.

3.2 Production History Matching

Prior to production history matching the initialization was performed by utilizing steady-state pressure, temperature, and fluid saturation conditions at the end of the initial state modeling. Production rate, brine injection rate and enthalpy, condensate injection rate and enthalpy were imposed as time-series inputs into the reservoir model. The total production and injection rates of wells were then distributed into each feed zone using mass allocation derived from historical PTS logs. The model was run throughout Salak commercial production operations including historical changes in major injection strategy consisting of 26 years of infield injection and recent injection realignment program implemented in Salak, Salak Injection Realignment Program (SIRP). The objectives of SIRP are to (1) reduce infield brine injection impact on two-phase production wells in western area of Salak, and (2) promote steam cap development through reservoir voidage increase. The SIRP has redistributed fractions of infield brine previously injected in AWI I to more distal injectors (AWI N & O) through proximal southeast (PSE) and to outfield area of Salak (AWI R) through brine outfield injection (BOI). Full SIRP implementation has commenced since Q2 2022, accompanied by comprehensive well and reservoir monitoring programs designed to carefully capture the reservoir's response to the SIRP. During production history matching, the calibration parameters included storage terms (porosity), matrix-fracture connectivity terms (matrix permeability, fracture spacing), and where required, flow terms (fracture permeability). In total, there were 60 wells employed as calibration constraints to match the evolution of liquid pressure, steam cap pressure, and flowing enthalpy.

The deep liquid pressures from shut-in PT data and liquid pressure monitoring wells are accurately reproduced across all production cells in Salak as appear in figure 10-11. AWI C-1 has served as a dedicated deep liquid pressure monitoring well since the first year of commercial production at Salak, providing a representation of the reservoir's historical pressure evolution. This history captures responses associated with several major changes in field operations, such as the commissioning of the additional 220 MW Units 3-6 in 1997 and, more recently, the injection-realignment project. During these periods, the observed downhole pressure data indicated higher liquid pressure declines associated with increased extraction following installation of new generating units and with increased net reservoir voidage resulting from injection realignment, both of which are well matched by the numerical model results.

Due to spatial variations in initial rock temperature and extraction rates, shallow steam cap reservoir exhibits strong pressure gradient, which allows its subdivision into three regimes, namely, low, medium, and high steam cap pressure. Calibration quality in these three regimes is demonstrated by very good agreement with actual shut-in PT and stable shut-in wellhead pressure (WHP) data in steam cap wells or wells with steam cap feed zone as depicted in figure 12 to 14. Recent field data after SIRP indicates moderation of production decline in several eastern steam cap wells. The production performance increase in those wells may be attributed to rapid flashing from the underlying high-temperature boiling zone following accelerated reservoir liquid level depletion, which effectively increases steam cap reservoir volume. This behavior has been captured by the numerical model, as evidenced by the moderating simulated steam cap pressure decline after SIRP in low to medium steam cap pressure wells located in eastern area. The last dynamic data used for calibrating the model is the flowing enthalpy, the flowing enthalpy from upstream (production wells) and downstream (power plant and injection wells) are utilized, figure 15 portrayed the Salak field wide enthalpy matching. Corresponding with drop in reservoir liquid level due to increase in net reservoir voidage after SIRP, flowing enthalpy in Salak has increased in agreement with numerical model result, confirming less infield brine injection cooling and/or accelerated steam cap expansion. Both value and trends of the flowing enthalpy were properly simulated indicating consistent reproduction of thermodynamic evolution within the reservoir.

Additionally, microgravity surveys provide an independent mass-balance constraint as it measured the actual net-mass changes or depletion in the reservoir due to steam saturation changes, natural recharge, etc. The example of microgravity matching in the period of 2005-2020 at several benchmarks in west, east, southwest, and northeast margin are shown in figure 16. Over the area with maximum change the mismatch ratio is still within +/- 10% of its observed value (Azimmah, 2023). Furthermore, the historical steam cap reservoir evolution area in the model were also confirmed by the density change model from geophysical monitoring. The decline in gravity is interpreted as density changes due primarily to the development of the two-phase zone where liquid saturation is lower in both the rock matrix and its fracture network (figure 17 left). This distribution of density changes in period 2011-2020 also agrees with the area of steam cap evolution in the numerical model (figure 17 right).

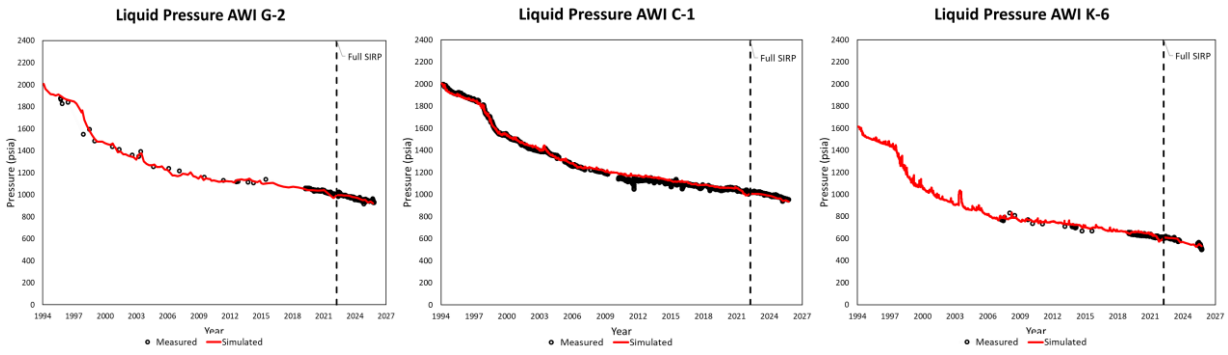

Figure 10: Liquid pressure match in the West and Central Production Cells, demonstrating good correspondence between simulated and measured pressures.

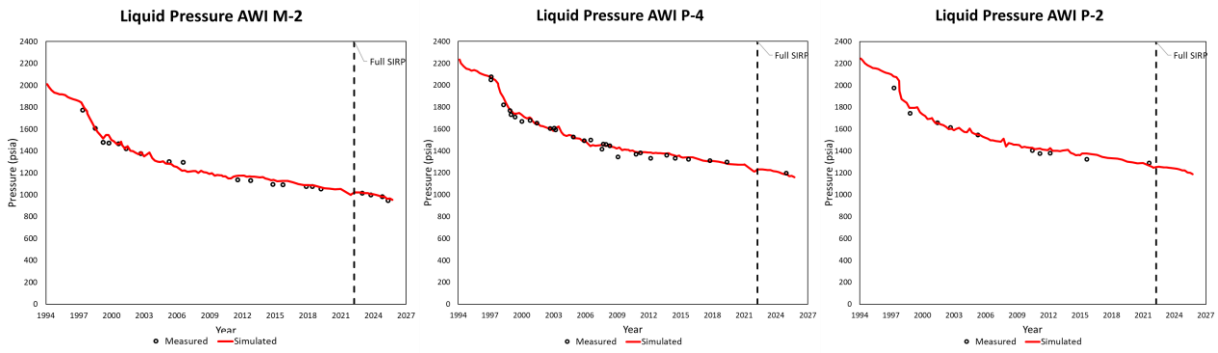

Figure 11: Liquid pressure match in the East Production Cells, demonstrating good correspondence between simulated and measured pressures.

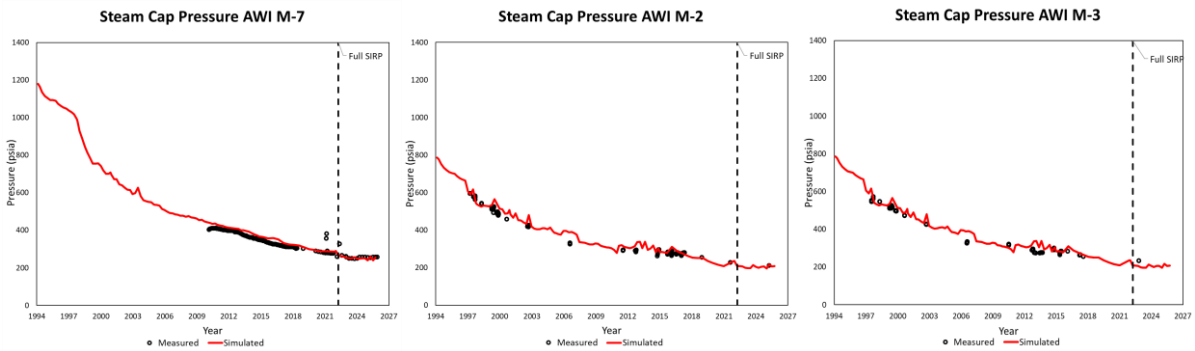

Figure 12: Low steam cap pressure match demonstrating accurate reproduction of observed pressure.

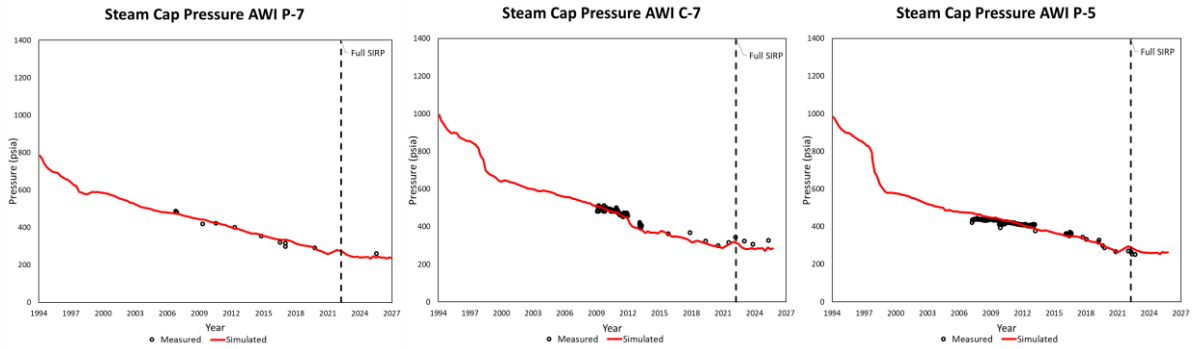

Figure 13: Medium steam cap pressure match demonstrating accurate reproduction of observed pressure.

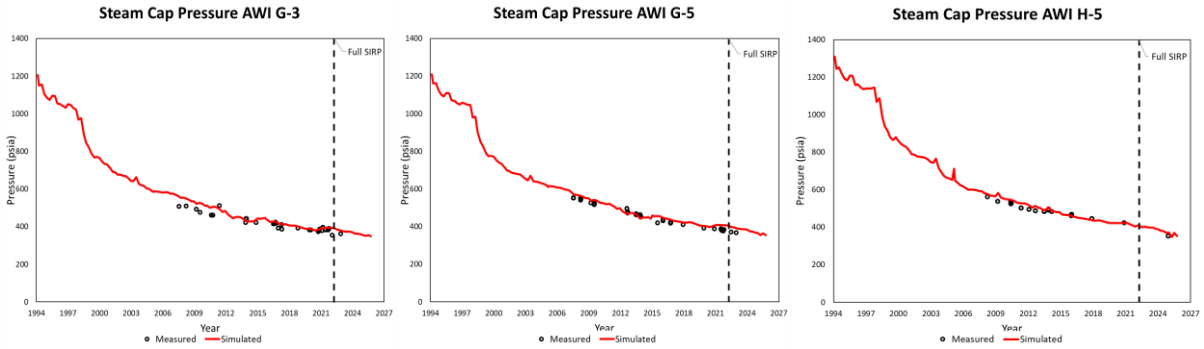

Figure 14: High steam cap pressure match demonstrates accurate reproduction of observed pressure.

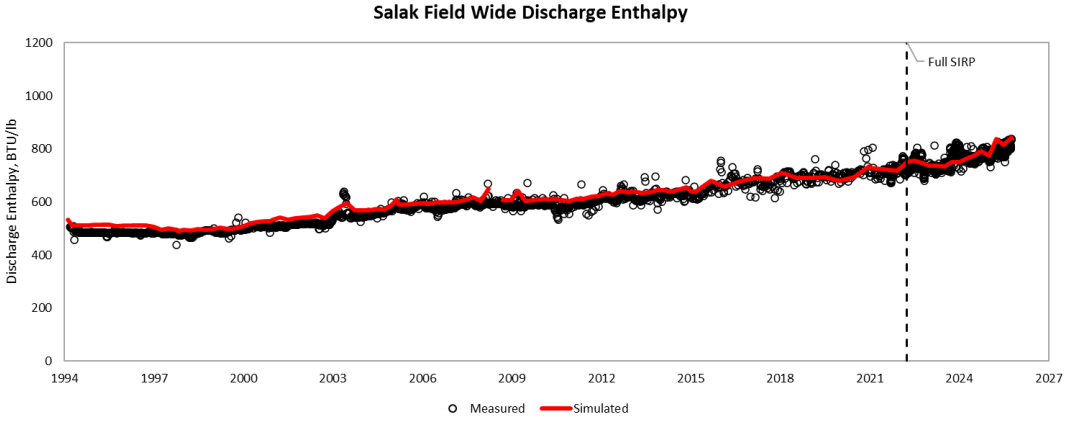

Figure 15: Field wide enthalpy evolution match between the simulated and measured data. The model successfully replicates the observed flowing enthalpy evolution.

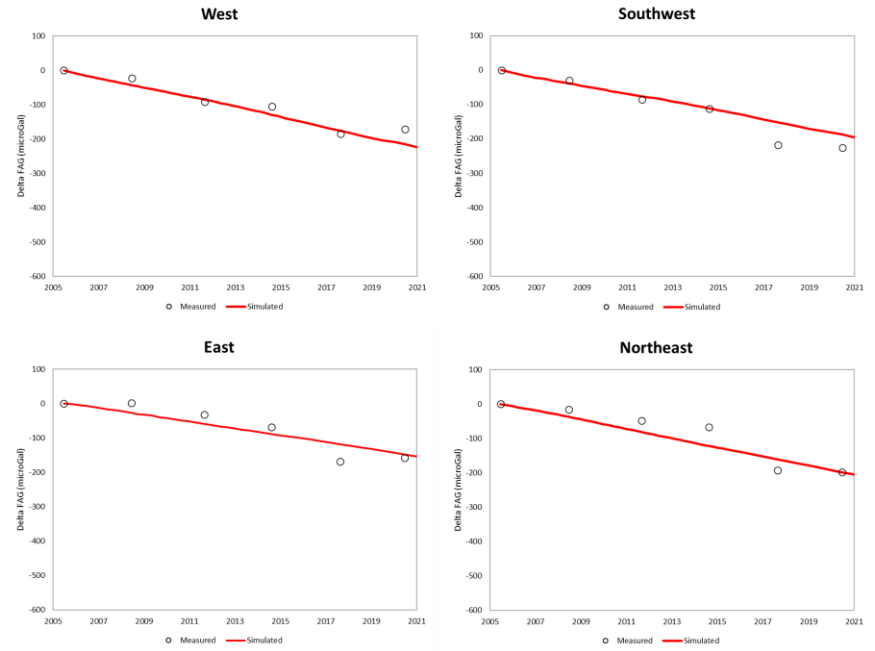

Figure 16: Microgravity matching at multiple benchmarks in Salak, providing constraints on the net mass balance in the current reservoir model.

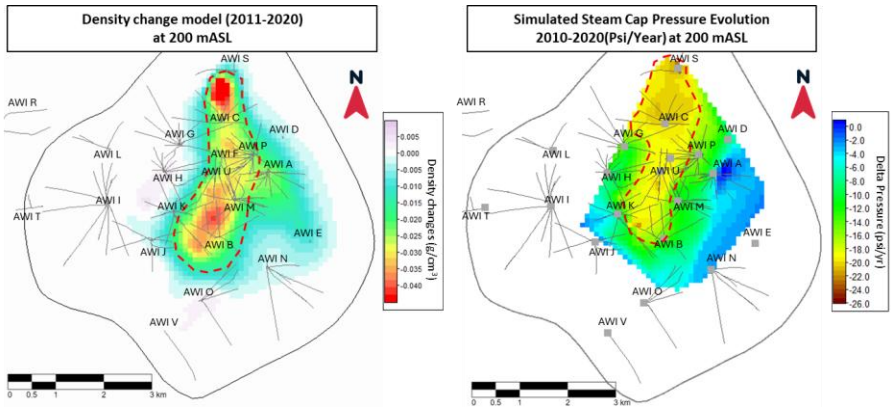

Figure 17: Good correspondence between modeled density changes and the simulated steam-cap pressure evolution.

4. NUMERICAL MODEL FORECAST

The numerical model forecasts at Star Energy Geothermal (SEG) were performed using an in-house program, TOUGHRunner. TOUGH Runner is a shell program that couples TOUGH2 with SEG's proprietary wellbore simulator (GEOFLOW) in forecast mode. At first, the program extracts the pressure and calculates the enthalpy based on the temperature and fluid saturation for each individual feed zone from the model. The reservoir pressures and enthalpies are then used to estimate the peak deliverability given operating WHP, well geometry, and PIs using GEOFLOW with the Duns and Ross correlations. The TOUGHRunner output includes time series of projected steam rate (convertible to electrical generation), brine rate, enthalpy and number of future infill wells required to sustain generation during the production plateau period.

Prior to performing the forecast, the productivity indices (PIs) of existing and new infill wells were calibrated. The PIs of the existing production wells were calibrated to match their historical deliverability, whereas the PIs of more than 100 new infill wells were also calibrated based on the averaged value and statistical distribution of production performance observed in the existing wells as indicated in Figure 18.

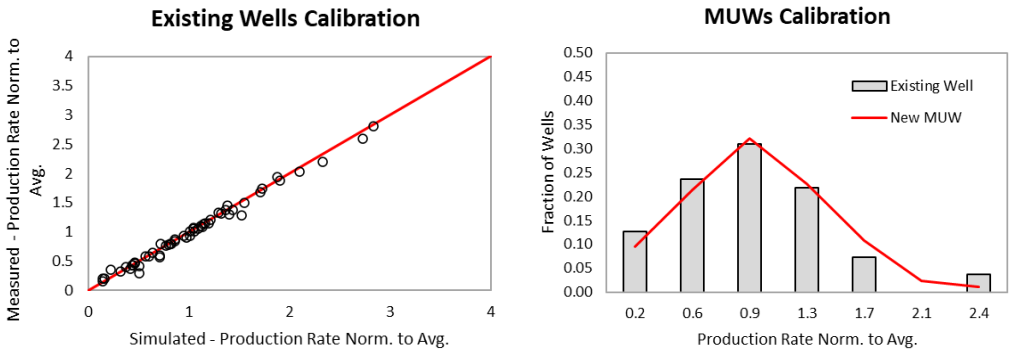

Figure 18: Calibration quality of existing well indicates good agreement with observed data, with most points clustered along the identity line (left chart). In addition, the production performance of new MUW also aligns with the mean and interquartile ranges from the existing wells (right chart).

Further validation was performed by utilizing the model to forecast the reservoir performance since the beginning of injection realignment. This assessment investigated the viability of injection realignment concept and its implications for well and reservoir behavior and compared these results with those expected under an in-field injection strategy. A reality check used as quality assurance of the model is the model's representation of short-term production decline without and with injection realignment. In the scenario without Salak Injection Realignment Program (SIRP), the model was run by keeping the injection of produced brine from western wells to AWI I (infield). In the SIRP scenario, portions of the brine produced from the western wells are redistributed to AWI N-O (edge field) and AWI-R (outfield). The results demonstrated that, in both cases, the model successfully reproduces the observed data including reservoir improvements as shown in the moderation of production decline following injection realignment. Furthermore, the forecasts also suggest that SIRP implementation could enhance long-term reservoir performance by reducing in-field injection-related cooling and promoting rapid steam cap development. These are reflected in the improved performance of production wells, which suggest higher liquid pressure drops due to voidage increase, followed by increase in flowing enthalpy in two-phase wells and a moderated steam cap pressure decline in dry steam wells, as depicted in Figure 19.

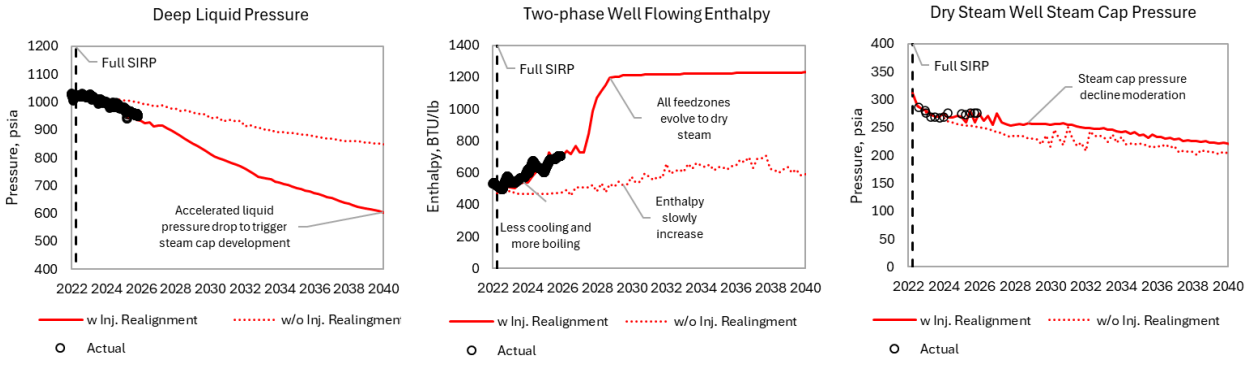

Figure 19: The model suggests that the implementation of Salak Injection Realignment Program (SIRP) would improve long-term reservoir performance as evidenced from actual data.

5. SUMMARY

The new numerical model of Salak field was constructed using an updated conceptual and static model as well as an improved fracture property distribution based on results from the naturally fractured reservoir study. The model has been calibrated against measured dynamic data from over 50-60 wells in pre-exploitation condition and reservoir response throughout commercial production. This includes the recent response following major injection realignment program, where the model successfully reproduced the observed evolution of key dynamic parameters. Calibration process was further strengthened by an independent validation of mass-balance changes derived from microgravity measurements. As part of further quality assurance, a short-term forecast was carried out to verify that the model accurately reproduces production decline without and with injection realignment program implementation. This high-quality numerical modeling effort provides a more realistic representation of Salak reservoir and enhances the confidence of the model to be used as an appropriate tool to forecast long-term field development and exploitation strategies. The model serves as a robust tool to assist Salak Asset Management Team and Star Energy Geothermal in improving the quality of the decisions made on strategic projects in Salak.

REFERENCES

Acuña, J., Astra, D., Molling, P., Prabowo, H., Stimac, J., and Sugiaman, F.: Awibengkok 1997 Conceptual Model Summary (edited by J. Stimac with contributions from W. Cumming, G. Nordquist, and J. Shemeta), UGI In-house Report (1997).

Acuña, J.A., Stimac, J., Sirad-Azwar, L., Pasikki, R.G.: Reservoir Management at Awibengkok Geothermal Field, West Java, Indonesia, Geothermics (2008).

Acuña, J.A..: Heat Transfer in Dual Porosity Systems, Unocal 76 In-House Report (1997).

Acuña, J.A..: Documentation on Dynamic Reservoir Simulation and Design of Experiment Analysis, CGI In-House Report (2009).

Aprilina, N.V., Putra, F.J., Wicaksono, S., Julinawati, T., Tanuwidjaja, R., Hernawan A.: Results of I-I Deep Well: Impact on the Conceptual Model of the Salak Geothermal System. PROCEEDINGS, The 5th Indonesia International Geothermal Convention & Exhibition 2017, Cendrawasih Hall - Jakarta Convention Center Indonesia (2017).

Aprilina, N., V., Putra, F., J., Golla, U., G., and Nordquist, G.: 3D Static Modeling Update of the Salak Geothermal Field, Indonesia: Earth Science-Defined Conceptual Features and Reservoir Properties for the New Numerical Model. WGC (2021).

Azimmah, A.: Observed Simulated Gravity Matching– 2021v265, SEGS In-house Report (2023).

Ganefianto, N., Stimac, J., Azwar, L.S., Pasikki, R., Parini, M., Shidarta, E., Joeristanto, A., Nordquist, G., Riedel, K.: Optimizing Production at Salak Geothermal Field, Indonesia, Through Injection Management. WGC (2010).

Golla, G.U., Julinawati, T., Putri, R.P., Nordquist, G., Libert, F., and Suminar, A.R.: The Salak Field, Indonesia: On to the next 20 years of production, Geothermics, 83, (2020).

Hulen, J.B., and Lutz, S.J.: Alteration Mineralogy and Zoning in Corehole AWI 1-2, Awibengkok Geothermal System, West Java, Indonesia, GRC Transactions, Vol. 23, pp 19-23, (1999).

Kurniawan, I., Peter., Hamdani., M. R.: 2021 Salak Numerical Model, SEGS In-House Report (2023).

Nordquist, G.: Fracture Permeability Anisotropy Study Results, Chevron Geothermal Resource Group In-house report (2017).

Pasikki, R., Hernawan, A.: Salak Reservoir Model, CGS In-House Report (2016).

Pasikki, R., Bratakusumah, B., Mulyadi: Numerical Model of Wayang Windu Geothermal System to Optimize Production Strategy, 7th IIGCE, Jakarta (2019).

Peter, Pasikki, R.: Salak BOI Project: Salak Reservoir Simulation Forecast, CGS In-House Report (2012).

Rahmansyah, F., Peter., Kurniawan., I.: 2020 Salak Reference Model Update, SEGS In-House Report (2020).

Rahmansyah, F., Peter.: 2018 Salak Reference Model Update, SEGS In-House Report (2018).

Rohrs, D., Gunderson, R., Melosh, G., Suminar, A., Nordquist, G., Molling, P., Sirad-Azwar, L., and Acuña, J.: Salak 2005 Conceptual Model Update, CGS In-house Report (2005).

Salak Asset Management Team: 2014 Salak State of the Reservoir. CGS In-House Report, October 15 (2015).

Salak Earth Science Team: Conceptual Model of Salak Geothermal Field, SEGS In-house report, September (2017).

Salak Reservoir Management Team: 1Q 2024 Salak Injection Realignment Program Update, SEGS In-house report (2024).

Stimac, J., Nordquist, G., Suminar, A. and Sirad-Azwar, L.: An Overview of the Awibengkok Geothermal System, Indonesia, Geothermics, 37 (2008), pp. 300-331.

Stimac, J. and Sugiaman, F.: The AWI 1-2 Core Research Program: Part I, Geologic Overview of The Awibengkok Geothermal Field, Indonesia, Proceedings 2000 World Geothermal Congress, Kyushu – Tohoku, Japan, (2000).

Strobel, C.: Awibengkok Project Resource Feasibility Update, UGI In-house Report (1986).